Journal of Materials Chemistry

Cite this: *J. Mater. Chem.*, 2011, **21**, 2609

www.rsc.org/materials

PAPER

Solid state NMR study on the thermal decomposition pathway of sodium amidoborane $NaNH_2BH_3$

Keiji Shimoda, Yu Zhang, Takayuki Ichikawa,* Hiroki Miyaoka and Yoshitsugu Kojima

Received 26th August 2010, Accepted 8th November 2010
DOI: 10.1039/c0jm02828b

The thermal decomposition pathway of sodium amidoborane (NaAB; $NaNH_2BH_3$) has been investigated in detail by using solid state NMR spectroscopy. ^{23}Na MAS/3QMAS NMR spectra suggested that NaH and an amorphous Na–N–B–H phase started to be formed as decomposition products even at 79 °C, although NaAB was prepared from NaH and NH_3BH_3 by ball milling at room temperature. Based on the quantitative analyses of the ^{23}Na MAS spectra, we proposed a decomposition reaction to 200 °C to be $NaNH_2BH_3 \rightarrow Na_{0.5}NBH_{0.5} + 0.5NaH + 2.0H_2$. The hypothetical phase $Na_{0.5}NBH_{0.5}$ is amorphous, where the basic molecular unit of the original NaAB is polymerized into a $[\text{–B}{=}\text{N–}]_n$ network structure. It was also found that the diammoniate of diborane (DADB) and polyaminoborane (PAB) were not formed during the decomposition of NaAB, which are both key compounds on the pyrolysis of ammonia borane (AB).

Introduction

The development of safe and economically viable on-board hydrogen storage materials for fuel cells is a crucial issue to achieve a hydrogen-based energy economy.[1] Recent research efforts have focused on chemical hydrogen storage consisting of light elements, which provides an advantage of high volumetric and gravimetric hydrogen capacity.[2,3] Much attention has been paid to ammonia borane (AB; NH_3BH_3) as one of the most promising candidates for effective hydrogen storage. AB contains 19.6 mass% H_2, and ~13 mass% of which can be released below 200 °C.[3] However, its practical application is greatly discouraged by the low dehydrogenation kinetics below 100 °C and by the concurrent release of toxic borazine, diborane, and ammonia above 145 °C.[4–7] Recently, metal amidoboranes (MAB), $LiNH_2BH_3$ and $NaNH_2BH_3$, have been reported as novel hydrogen storage materials,[8] which are the AB derivatives replacing one H^+ by M^+, where the cation M^+ acts as charge-balancer in MAB, $M^+[NH_2BH_3]^-$.[9] They release 10.9 and 7.5 mass% H_2, respectively, at significantly lower temperatures (~90 °C) without any release of borazine and diborane.[8] Although the subsequent related studies have made great efforts to clarify the dehydrogenation reaction mechanism of the MAB,[6,10–13] they are partly unsuccessful because the decomposition products are difficult to characterize due to their amorphous(-like) feature. Nuclear magnetic resonance (NMR) spectroscopy is a useful technique to characterize such multi-component amorphous materials. Although ^{11}B NMR has been effectively utilized in some of the previous works,[6,12,13] these studies only focused on a given temperature and are difficult to fully characterize the decomposition pathway of the MAB. Here, we have reinvestigated, in detail, the thermal decomposition of sodium amidoborane (NaAB; $NaNH_2BH_3$) using ^{11}B and ^{23}Na MAS/3QMAS NMR techniques, in combination with a discussion of thermal gas desorption properties.

Institute for Advanced Materials Research, Hiroshima University, 1-3-1 Kagamiyama, Higashi-Hiroshima, 739-8530, Japan. E-mail: tichi@hiroshima-u.ac.jp; Fax: +81-82-424-5744; Tel: +81-82-424-5744

Experimental section

The starting materials NaH (purity 95%) and NH_3BH_3 (90%) were purchased from Sigma-Aldrich Co. Ltd., and were used as-received without further purification. All the samples were handled in an Ar-purified glove box with the oxygen and water contents of <1.0 ppm. NaAB was prepared by a ball milling technique.[8] The reagent mixture of NaH and NH_3BH_3 with a molar ratio of 1 : 1 was put into a Cr-steel vessel with 20 steel balls (ball-to-sample weight ratio is 100 : 1), and then milled at 200 rpm for 1 h under 1 MPa hydrogen atmosphere by a Fritsch-P7 planetary milling apparatus. The prepared sample was characterized by X-ray diffraction with the Cu Kα radiation (XRD; RINT-2100, Rigaku Co. Ltd.) to confirm the successful synthesis of NaAB.

The thermal gas desorption properties were examined by thermogravimetry-differential thermal analysis (TG-DTA; TG8120, Rigaku Co. Ltd.) coupled with quadrupole mass spectrometry (MS; M-QA200TS, Anelva Co. Ltd.) upon heating to 200 °C under a He flow. The flow rate was 300 cm^3 min^{-1} and the heating ramp was 1 °C min^{-1}.

^{11}B and ^{23}Na magic-angle spinning (MAS), cross-polarization (CP) MAS, and triple-quantum (3Q) MAS NMR spectra were recorded on a JNM-ECA600 spectrometer (JEOL Co. Ltd.) in a magnetic field of 14.1 T with the ^{11}B resonant frequency of 192.5 MHz. Sample powders were packed into 4 mm ZrO_2 rotors under an Ar atmosphere, which were spun at a speed of 15 kHz. Chemical shifts were referenced to saturated H_3BO_3 aqueous solution at 19.49 ppm for ^{11}B, and 1 M NaCl solution at 0.00 ppm for ^{23}Na, respectively. Single pulse MAS spectra were acquired with the optimized pulse widths of 1.5–2.0 μs (90°-flip angle) and relaxation delays of 5–10 s for ^{11}B, and 1.75–2.0 μs for ^{23}Na, respectively, to ensure their quantitativeness. 3QMAS measurements were carried out with a conventional z-filter sequence,[14] and the free induction decay (FID) signals were Fourier-transformed and sheared to obtain two-dimensional spectra, from which the isotropic chemical shift δ_{iso} and quadrupolar product P_q were estimated.[15] All the spectra were acquired at room temperature.

Results and discussion

Fig. 1 represents the TG-DTA curve (a) and the thermal gas desorption properties (b) for NaAB. The TG curve indicated that the onset of the sample weight loss is around 60 °C and the weight drastically decreases between 80 and 90 °C. Another weight loss with a different slope was seen above 90 °C. We note that the TG curve obtained in this study was similar to that reported by Xiong *et al.*,[10] but slightly different from that of Fijałkowski and Grochala.[12] The DTA curve showed a sharp exothermic peak at 84–85 °C, which is also consistent with the previous studies.[8,10,12] It is noted that sharp peaks at 84 °C in the DTA curve and the MS profile for H_2 were deformed due to the rapid exothermic reaction of NaAB. In the thermal gas desorption profile, a large amount of hydrogen was released at 84 °C which was followed by the second desorption above 115 °C. The hydrogen desorption correlates with the TG curve, suggesting that the sample weight loss was attributable to hydrogen release with increasing temperature. It should be noted that a very small amount of ammonia was also detected concomitantly with the first hydrogen release as shown in Fig. 1(b). The ammonia release was not noted in the previous studies,[8,10] but consistent with Fijałkowski and Grochala.[12] The other impurities such as diborane (B_2H_6) and borazine ($(HNBH)_3$) were not observed, indicating no possibility of the presence of unreacted AB in the ball milled sample.

^{11}B MAS NMR spectra of AB and the as-prepared NaAB are compared in Fig. 2. AB and NaAB have a peak at −25.4 ppm and −22.9 ppm, respectively. Both the samples have a single

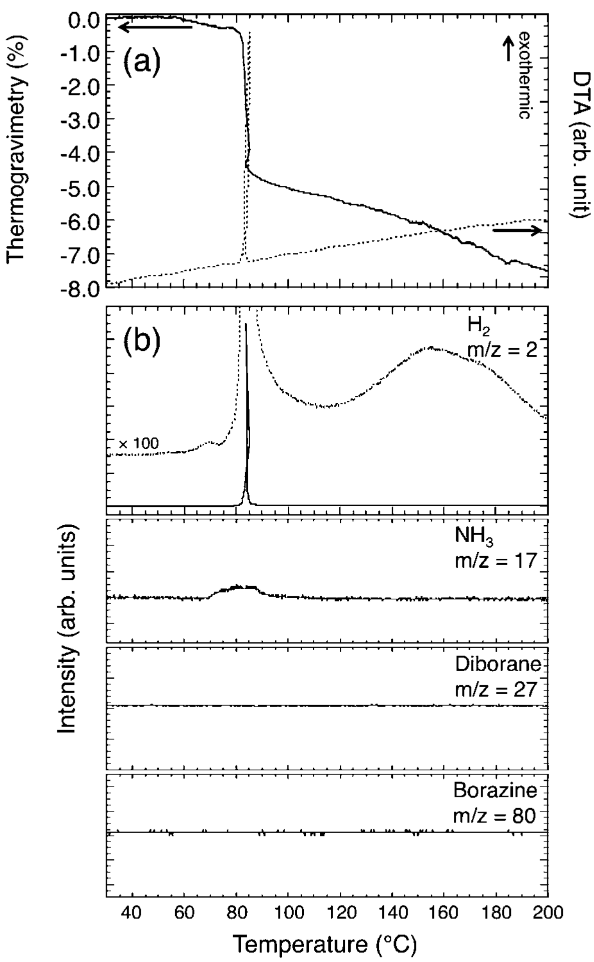

Fig. 1 (a) TG-DTA curves and (b) thermal gas desorption profiles (H_2, NH_3, B_2H_6, and $(HNBH)_3$) of NaAB up to 200 °C. It should be noted that sharp peaks at 84 °C in the DTA curve and the MS profile for H_2 were deformed due to rapid exothermic reaction of NaAB.

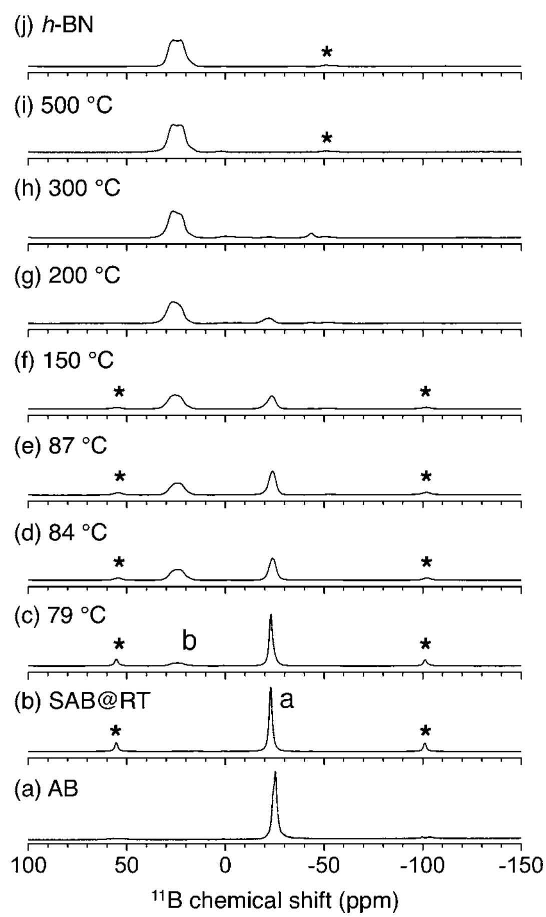

Fig. 2 ^{11}B MAS NMR spectra of (a) as-received AB and NaAB at (b) room temperature, (c) 79 °C, (d) 84 °C, (e) 87 °C, (f) 150 °C, (g) 200 °C, (h) 300 °C, (i) 500 °C, and (j) *h*-BN milled under Ar for 1 h (reference). Spinning sidebands are indicated by asterisks.

boron site ([NBH_3]),[8,16] indicating that the asymmetric peak shape of AB is influenced by the nuclear quadrupolar interaction. The small difference in chemical shift indicates the small difference in the chemical environment of the boron atom in NH_3BH_3 and $NaNH_2BH_3$. Fig. 2 also shows the ^{11}B MAS spectra of NaAB at different temperatures during the decomposition process. By increasing the temperature to 79 °C, an additional broad peak was observed at 25 ppm (peak B). This broad peak grew and finally became dominant above 200 °C as shown in Fig. 2. This peak can be assigned to three-fold boron ([BN_3] or [N_2BH] species) as in hexagonal BN (*h*-BN) or polyborazilene.[17] Moreover, the ^{11}B CPMAS measurement for the sample at 150 °C indicates that the boron atom, attributed to the peak b, is spatially close to hydrogen, suggesting the presence of the [N_2BH] species as in polyborazilene. ^{11}B 3QMAS spectrum of the decomposition product at 200 °C (Fig. 3) indicated that the peak b showed a quadrupolar lineshape with a δ_{iso} of 31 ppm and a large P_q of 3.3 MHz, which is in reasonable agreement with those for the [N_2BH] species in polyborazilene.[17] It is also interesting to note that the NBH_3 peak at −23 ppm (peak a) in Fig. 2 became broader above 84 °C. This indicates that the NBH_3 species are in an amorphous state above the onset of H_2 desorption. By increasing the temperature to 200 °C, the NBH_3 peak became weaker and finally disappeared above 300 °C. We note that, in addition to the three-fold boron species, small amounts of [$N_3BH + N_2BH_2$] (−10–0 ppm) and [BH_4] (−44 ppm) units[12,18,19] were also observed above 200 °C.

Fig. 4 shows ^{23}Na MAS spectra of NaAB at different temperatures during the decomposition process. At room temperature, a complex signal with two peaks was observed (peak A). This lineshape seems to result from a large quadrupolar interaction on a single Na site in NaAB,[8] which will be discussed later. At the onset of dehydrogenation (79 °C), a sharp peak was observed at 17.6 ppm (peak B), which increased in intensity with increasing temperature up to 300 °C. This peak is assigned to NaH, indicating that NaH is formed from just above the onset temperature for H_2 desorption. It should be noted that a small amount of NaH was already seen at room temperature, probably a remnant of the starting material. On the other hand, the quadrupolar lineshape of NaAB broadened above 84 °C, which is again consistent with the amorphization of NaAB. This broad peak shifted to slightly higher frequency and decreased in intensity as the temperature was increased up to 300 °C. At 300 °C, another peak was observed at ~1140 ppm (not shown), which is attributable to the Knight shift of Na metal formed by the decomposition of NaH. Then, most of the ^{23}Na signal disappeared at 500 °C due to the evaporation of the Na metal (not shown).

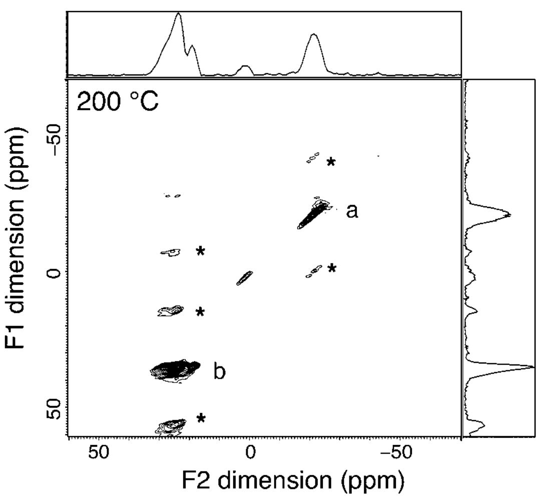

Fig. 3 ^{11}B 3QMAS NMR spectrum for the decomposition product of NaAB at 200 °C. The one-dimensional spectrum projected onto the F2 dimension corresponds to the MAS spectrum. The lateral spectrum is the projection onto the F1 dimension, where the second-order quadrupolar interaction is cancelled out. Spinning sidebands are indicated by asterisks.

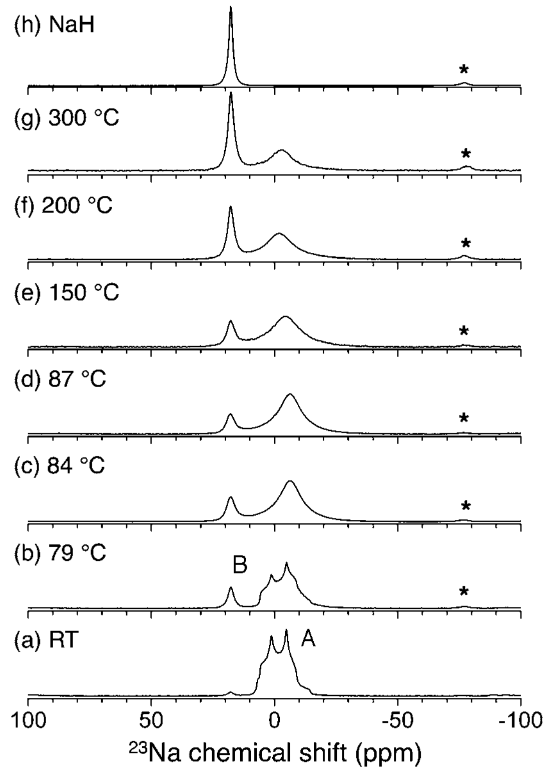

Fig. 4 ^{23}Na MAS NMR spectra of NaAB at (a) room temperature, (b) 79 °C, (c) 84 °C, (d) 87 °C, (e) 150 °C, (f) 200 °C, (g) 300 °C, and (h) NaH as a reference. Spinning sidebands are indicated by asterisks.

To obtain the detailed information on the Na environment, ^{23}Na 3QMAS spectra were also acquired at different temperatures. The ^{23}Na 3QMAS spectrum at room temperature clearly shows the NaAB peak (peak A) characteristic of having the large quadrupolar interaction, which is cancelled out in the isotropic (F1) projection (Fig. 5(a)). The δ_{iso} and P_q values were estimated to be 7 ppm and 3.2 MHz, respectively. At 79 °C, the NaH peak (peak B; $\delta_{iso} = 18$ ppm) and an unknown peak (peak C; $\delta_{iso} \approx -5$ ppm), which had already appeared at room temperature, became significant in addition to the NaAB peak (Fig. 5(b)). The NaAB peak lost its quadrupolar lineshape above 87 °C (denoted as peak A′), and the unknown peak C became less significant up to 150 °C and finally disappeared at 200 °C (Fig. 5(c)–(e)). We note that peak C is relatively close in position to that of $NaBH_4$ ($\delta_{iso} = -4$ ppm) but totally different from that of $NaNH_2$ ($\delta_{iso} = 35$ ppm), although the presence of $NaBH_4$ is ruled out below 150 °C

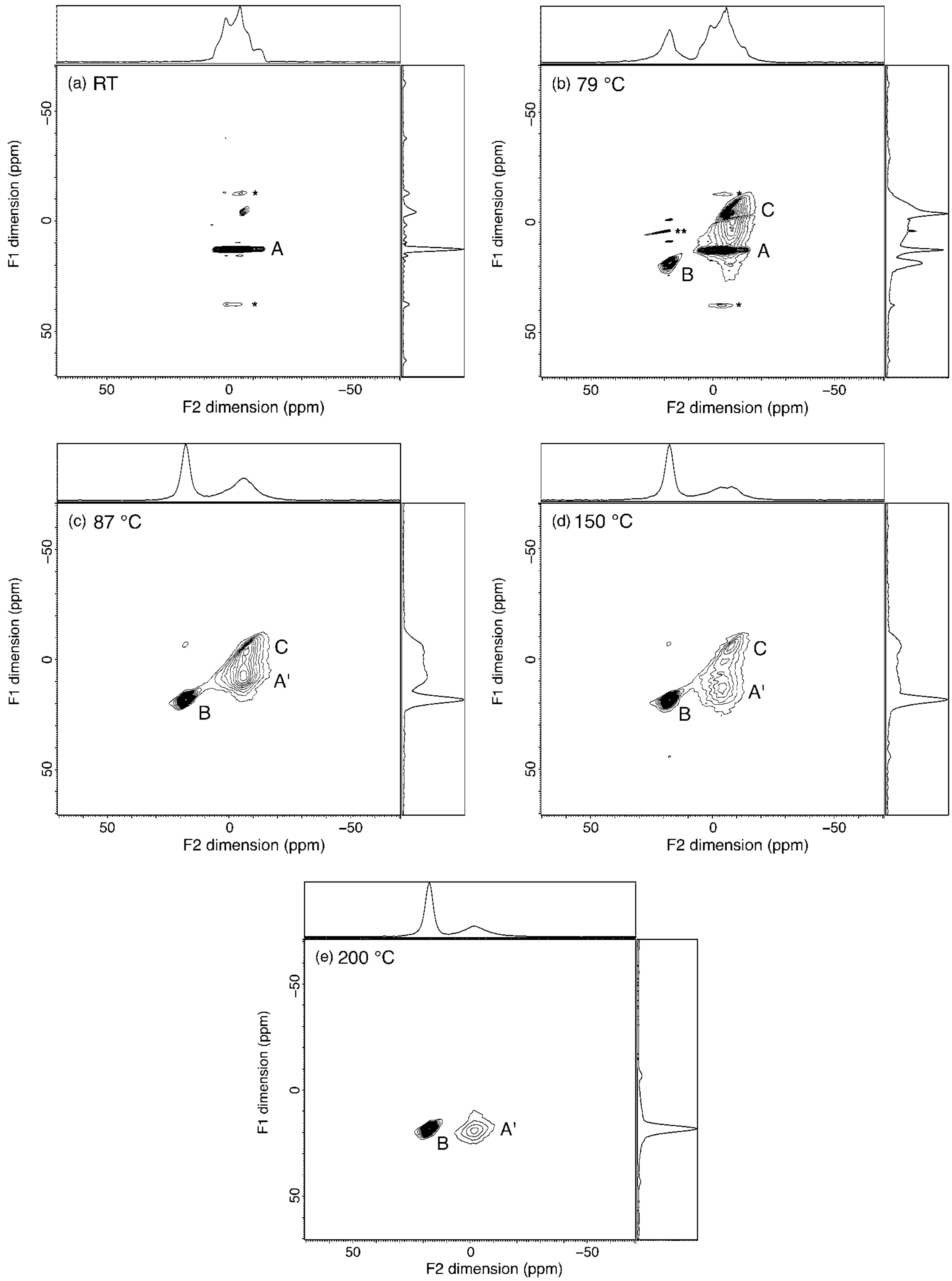

Fig. 5 ^{23}Na 3QMAS NMR spectra of NaAB at (a) room temperature, (b) 79 °C, (c) 87 °C, (d) 150 °C, and (e) 200 °C. The one-dimensional spectrum projected onto the F2 dimension corresponds to the MAS spectrum. The lateral spectrum is onto the F1 dimension, where the second-order quadrupolar interaction is cancelled out. Spinning sidebands are indicated by asterisks. A signal marked by double asterisk in (b) is an artifact.

by the ^{11}B MAS spectra. Finally, two signals coming from NaH and a NaAB-like site (peak A′; the δ_{iso} slightly shifted to 11 ppm), which will be discussed later, were observed at 200 °C (Fig. 5(e)).

Fig. 6 plots the peak intensity ratios of three-fold boron ([BN_3] or [N_2BH]) and NaH in the ^{11}B MAS and ^{23}Na MAS spectra as a function of temperature. The peak areas were integrated including all the spinning side bands over several hundred ppm. The intensity of [NBH_3] in the ^{11}B MAS spectra decreased above 79 °C and finally disappeared at 300 °C in parallel with an increase in three-fold boron (Fig. 6(a)). At 500 °C, almost all the boron atoms were converted into the three-fold species. Fig. 6(b) and (c) suggest that the formation of the three-fold boron and

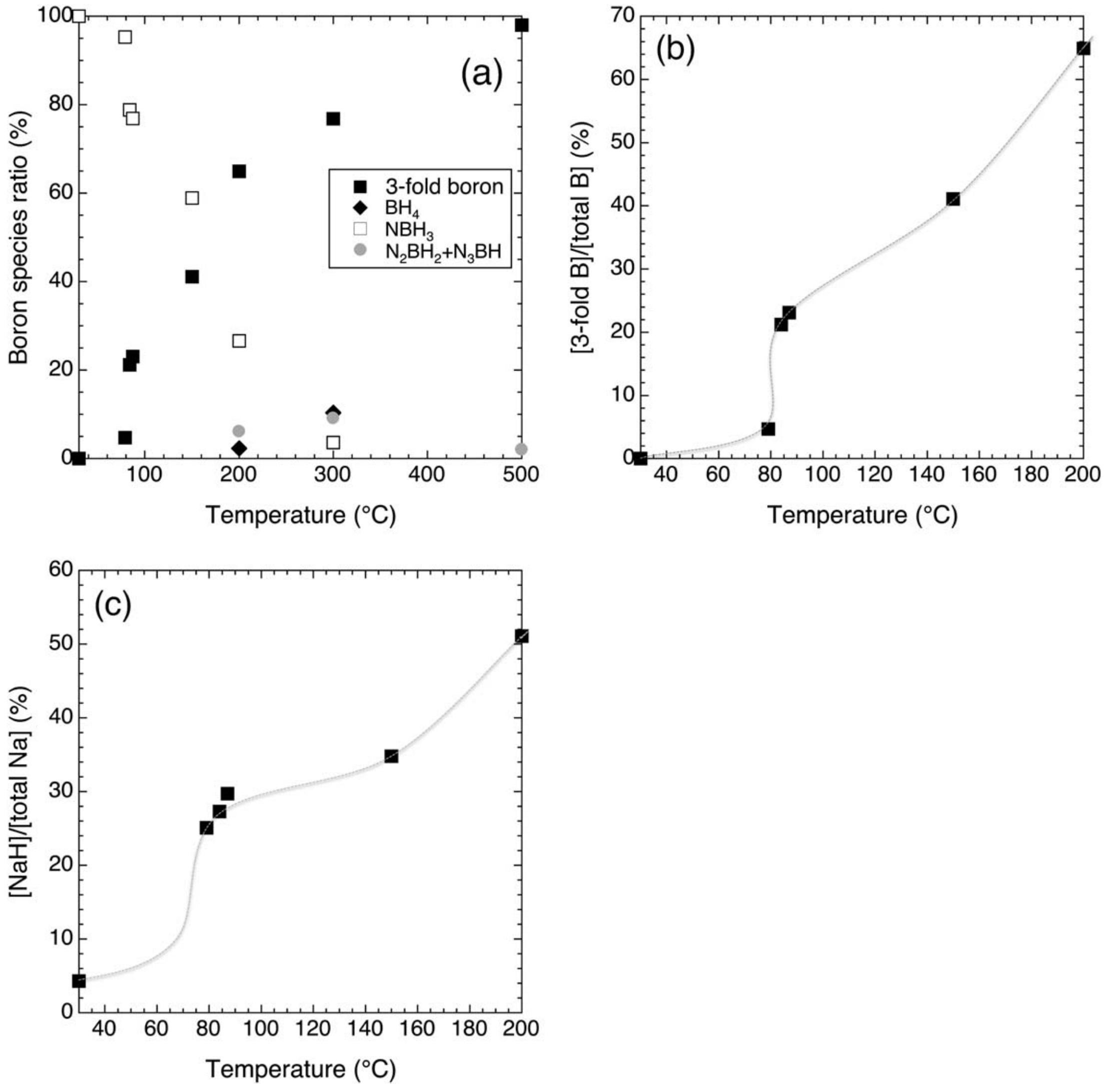

Fig. 6 Peak intensity ratios of (a) boron species (3-fold B ($[BN_3 + N_2BH]$), $[BH_4]$, $[NBH_3]$, and $[N_2BH_2 + N_3BH]$) as a function of temperature up to 500 °C, (b) 3-fold B species with respect to the total amount of B, and (c) NaH with respect to the total amount of Na as a function of temperature up to 200 °C. Lines are guides for the eyes.

NaH follows the two-step decomposition as shown in TG/MS curves.

Here, the thermal decomposition pathway of NaAB is discussed. Assuming that the amount of ammonia desorption was negligible (not a crucial reaction path), the sample weight loss was attributable to hydrogen released during the thermal decomposition of NaAB. According to the TG/MS results, the pyrolysis of NaAB can be separated into two stages. The first decomposition stage includes steep hydrogen release (60–115 °C). Based on the ^{11}B and ^{23}Na MAS/3QMAS NMR results, it is suggested that $Na^+[NH_2BH_3]^-$ molecules in NaAB start to polymerize by the intermolecular reaction between Na^+ or H^+ in a $Na^+[NH_2BH_3]^-$ molecular unit and H^- in the adjacent molecule at the beginning of dehydrogenation as follows,

$$[NaNH_2BH_3]_n \rightarrow NaNH_2[BHNH]_{n-1}BH_3 + (n-1)NaH + (n-1)H_2 \quad (1)$$

and

$$[NaNH_2BH_3]_n \rightarrow NaNH_2[BHNNa]_{n-1}BH_3 + 2(n-1)H_2. \quad (2)$$

These possible reactions yield the three-fold boron $[N_2BH]$ with consumption of the terminal $[NBH_3]$ unit by the polymerization as shown in Fig. 7. As a possible model for this polymerization, a chain-like –B=N– bond can be created (Fig. 7(a)), which is similar to polyiminoborane (PIB),[20] along with the formation of NaH (in reaction (1)) and H_2 gas release. This is

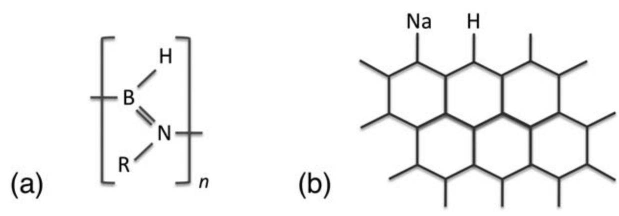

Fig. 7 (a) Proposed polymerization of $NaNH_2BH_3$ molecules (R denotes Na or H), and (b) a possible BN benzene-like ring formation.

similar to that proposed by the *ab initio* molecular orbital calculation.[11] As another model, the BN benzene-like ring structure as in *h*-BN or polyborazilene can also be considered (Fig. 7(b)). We speculate that the drastic hydrogen release at the first decomposition stage is a result of the "cooperative" polymerization between the $Na^+[NH_2BH_3]^-$ molecular units. At 115 °C, the weight loss reaches 5.3 mass%, which corresponds to 2.8 equiv. H of NaAB. Although the hypothetical chemical formula is given as $NaNH_{0.6}BH_{1.6}$, the results in this study strongly indicate that there is phase separation into NaH and a complicated amorphous material during H_2 desorption. The fact that NaH was formed above 79 °C, as one of the decomposition products of NaAB, is quite interesting because NaAB was prepared by ball milling NaH and AB at room temperature. Thus, the state including NaH is thermodynamically stable above 79 °C, meaning that NaH is isolated again during the decomposition process. Considering the amount of NaH estimated from Fig. 6(c), the decomposition pathway up to 115 °C can be written as

$$NaNH_2BH_3 \rightarrow Na_{0.7}NBH_{1.9} + 0.3NaH + 1.4H_2. \quad (3)$$

Here, the hypothetical $Na_{0.7}NBH_{1.9}$ is amorphous, which has a partially polymerized structure as proposed above (Fig. 7(a) and (b)).

The second decomposition stage can be identified from 115 to 200 °C with a relatively mild hydrogen release. The weight loss reaches 7.5 mass% at 200 °C. This corresponds to a 3.9 equiv. H of NaAB, implying that the main decomposition product is a tentative material "NaNBH"[8] or NaH/BN mixture.[10] Again, we should stress the presence of NaH and another amorphous material, based on ^{23}Na MAS NMR spectra. The presence of NaH is also confirmed by XRD, being consistent with the previous report.[10] These two phases have an almost equal amount of Na atoms at 200 °C (Fig. 6(c)). Therefore, we conclude that the decomposition pathway up to 200 °C would be expressed by the following reaction;

$$NaNH_2BH_3 \rightarrow Na_{0.5}NBH_{0.5} + 0.5NaH + 2.0H_2. \quad (4)$$

This suggests that $Na_{0.7}NBH_{1.9}$ changes to $Na_{0.5}NBH_{0.5}$ by releasing additional NaH and H_2 between 115 and 200 °C. The hypothetical material $Na_{0.5}NBH_{0.5}$ is also amorphous and may be considered as a mixture of *h*-BN and NaNBH-like structures, both of which contain three-fold boron. Its structural framework would be composed of BN benzene-like rings as in *h*-BN or $[\text{–B=N–}]_n$ chains similar to PIB, $(NHBH)_n$.[20] The unknown broad peak at −2 ppm on the ^{23}Na MAS NMR spectra at 200 °C (or peak A′ in Fig. 5(e)) corresponds to the Na environments in $Na_{0.5}NBH_{0.5}$. Finally, this phase would further decompose into *h*-BN and Na metal (and H_2 gas) above 500 °C.

NaAB ($NaNH_2BH_3$) is a derivative of AB (NH_3BH_3). Therefore, it may be useful to compare the decomposition pathways of the two materials. The decomposition mechanism of AB has been investigated using *in situ* ^{11}B MAS NMR spectroscopy up to 88 °C.[19] The formation of DADB (diammoniate of diborane; $[(NH_3)_2BH_2]^+[BH_4]^-$) precedes the decomposition of AB. This material contains $[N_2BH_2]$ and $[BH_4]$ species, which have the chemical shifts of −13 ppm and −38 ppm, respectively. The ^{11}B MAS spectra obtained in this work did not show any evidence of such species below 200 °C, indicating the absence of DADB-like dimer molecules during the decomposition of NaAB. Above 112 °C, AB releases hydrogen and is polymerized to PAB (polyaminoborane; $(NH_2BH_2)_n$), which contains $[N_2BH_2]$.[4,19,20] PAB changes into PIB (polyiminoborane; $(NHBH)_n$) with further hydrogen release (and non-negligible amounts of ammonia, diborane and borazine) above 145 °C.[4–7] The molecular structure of PIB is believed to be an infinite chain of $[\text{–B=N–}]_n$ where the boron is in the three-fold coordination ($[N_2BH]$).[20] Finally, the chain structures of PIB are also polymerized to BN benzene rings as in *h*-BN by exhausting hydrogen at 500–600 °C.[4] Based on the NMR study, NaAB does not pass through PAB as a transient phase, but directly transforms into *h*-BN- and/or PIB-like structure. The absence of PAB may be the key to the absence of the release of toxic gases, diborane and borazine, on the thermal decomposition of NaAB.

Conclusions

We have reinvestigated the thermal decomposition pathway of sodium amidoborane (NaAB; $NaNH_2BH_3$) by using TG/MS and solid state NMR spectroscopy. The TG/MS profiles showed the two-step decomposition up to 200 °C. The first stage started from ~60 °C, accompanying a drastic H_2 release. A small amount of NH_3 was also detected in the first stage as recently reported. The second stage was identified from 115 °C to 200 °C. In this stage, the H_2 desorption was relatively mild. At 200 °C, the weight loss reaches 7.5 mass%, corresponding to ~2.0 H_2 release per $NaNH_2BH_3$. On the basis of ^{23}Na NMR results, the formation of NaH and an unidentified amorphous Na–N–B–H phase was clearly formed above 80 °C. The Na–N–B–H phase should have a $[\text{–B=N–}]_n$ polymerized network, where the boron is in the three-fold coordination. We here underscore the usefulness of multinuclear (^{11}B and ^{23}Na) NMR technique with high magnetic field (> 14 T) to investigate the thermal decomposition pathway of light element-based hydrogen storage materials.

Acknowledgements

This work was partially supported by the NEDO project "Advanced Fundamental Research Project on Hydrogen Storage Materials".

References

1 L. Schlapbach and A. Züttel, *Nature*, 2001, **414**, 353.
2 W. Grochala and P. P. Edwards, *Chem. Rev.*, 2004, **104**, 1283.
3 P. Chen and M. Zhu, *Mater. Today*, 2008, **11**, 36.
4 M. G. Hu, R. A. Geanangel and W. W. Wendlandt, *Thermochim. Acta*, 1978, **23**, 249.
5 V. Sit, R. A. Geanangel and W. W. Wendlandt, *Thermochim. Acta*, 1987, **113**, 379.
6 X. Kang, Z. Fang, L. Kong, H. Cheng, X. Yao, G. Lu and P. Wang, *Adv. Mater.*, 2008, **20**, 2756.
7 K. Shimoda, unpublished datum.
8 Z. Xiong, C. K. Yong, G. Wu, P. Chen, W. Shaw, A. Karkamkar, T. Autrey, M. O. Jones, S. R. Johnson, P. P. Edwards and W. I. F. David, *Nature Mat.*, 2008, **7**, 138.
9 M. Ramzan, F. Silvearv, A. Blomqvist, R. H. Scheicher, S. Lebègue and R. Ahuja, *Phys. Rev. B*, 2009, **79**, 132102.

10 Z. Xiong, G. Wu, Y. S. Chua, J. Hu, T. He, W. Xu and P. Chen, *Energy Environ. Sci.*, 2008, **1**, 360.
11 D. Y. Kim, N. J. Singh, H. M. Lee and K. S. Kim, *Chem. Eur. J.*, 2009, **15**, 5598.
12 K. J. Fijałkowski and W. Grochala, *J. Mater. Chem.*, 2009, **19**, 2043.
13 A. T. Luedtke and T. Autrey, *Inorg. Chem.*, 2010, **49**, 3905.
14 J.-P. Amoureux, C. Fernandez and S. Steuernagel, *J. Magn. Reson.*, 1996, **A123**, 116.
15 J.-P. Amoureux, C. Huguenard, F. Engelke and F. Taulelle, *Chem. Phys. Lett.*, 2002, **356**, 497.
16 W. T. Klooster, T. F. Koetzle, P. E. M. Siegbahn, T. B. Richardson and R. H. Crabtree, *J. Am. Chem. Soc.*, 1999, **121**, 6337.
17 C. Gervais and F. Babonneau, *J. Organomet. Chem.*, 2002, **657**, 75.
18 M. E. Bluhm, M. G. Bradley, R. Butterick III, U. Kusari and L. G. Sneddon, *J. Am. Chem. Soc.*, 2006, **128**, 7748.
19 A. C. Stowe, W. J. Shaw, J. C. Linehan, B. Schmid and T. Autrey, *Phys. Chem. Chem. Phys.*, 2007, **9**, 1831.
20 D. Jacquemin, *J. Phys. Chem. A*, 2004, **108**, 9260.